



# Synthesis, characterization and swelling behavior of high-performance antimicrobial amphoteric hydrogels from corn starch

Nahed A. Abd El-Ghany<sup>1</sup> · Zain M. Mahmoud<sup>1</sup>

Received: 5 June 2020 / Revised: 1 September 2020 / Accepted: 13 October 2020 /

Published online: 19 October 2020

© Springer-Verlag GmbH Germany, part of Springer Nature 2020

## Abstract

Three novel hydrogels with high antimicrobial activity were synthesized from grafting of corn starch with 4-acrylamidobenzoic acid (4ABA) and diallyldimethylammonium chloride as cross-linkers (CLs). Three concentrations of the cross-linker (3%, 5% and 10% based on starch weight) were used to give three hydrogels designated as St-g-P4ABA/PCL3, St-g-P4ABA/PCL5 and St-g-P4ABA PCL10, respectively. The structure of the prepared hydrogels was evidenced by FTIR, <sup>1</sup>H-NMR, XRD and SEM techniques. The thermal stability as well as the swelling behavior of the starch hydrogels was investigated, and the results revealed high thermal stability and potential swell ability in water and 9% saline solution for the hydrogels compared with the native starch. They showed a higher swelling degree in acidic, basic and neutral buffer solutions; lower degradation was observed in acidic and basic media after 96 h. Starch hydrogel's antimicrobial activity actions against various types of gram-positive bacteria, gram-negative bacteria and fungi demonstrated higher growth inhibition ability against all tested microorganisms compared to zero-native starch inhibitions. The hydrogels did not demonstrate cytotoxicity on normal human cells and can therefore be used safely in pharmaceutical applications and drug delivery systems.

---

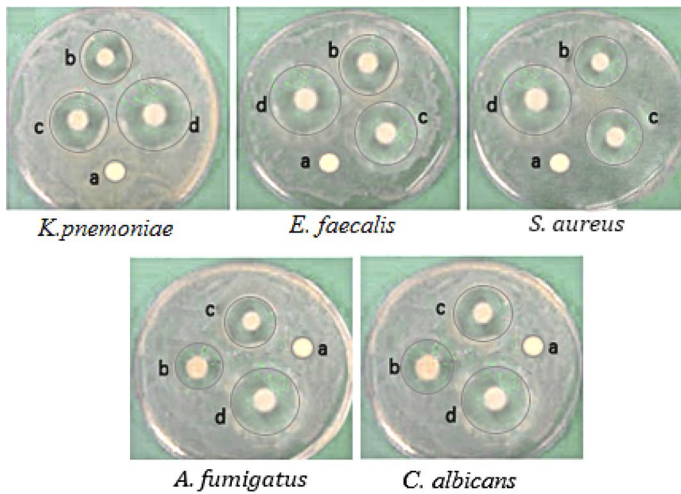
**Electronic supplementary material** The online version of this article (<https://doi.org/10.1007/s00289-020-03417-8>) contains supplementary material, which is available to authorized users.

---

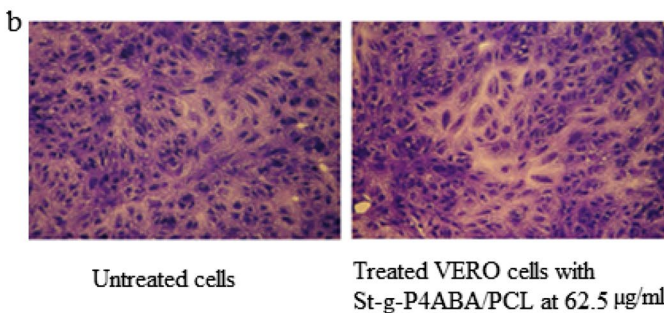
✉ Nahed A. Abd El-Ghany  
dr\_nahed\_055@yahoo.com

<sup>1</sup> Chemistry Department, Faculty of Science, Cairo University, Giza 12613, Egypt

## Graphic abstract



Normal photographs for the antimicrobial behavior of free starch (a), St-g-P4ABA/PCL3 (b), St-g-P4ABA/PCL10 (c) against *E. faecalis* and *S. aureus* as gram-positive bacteria; against *K. pneumoniae* as gram-negative bacteria in comparison with the antibacterial standard drug ciprofloxacin (d) and against *A. fumigatus* and *C. albicans* as fungi in comparison with the antifungal standard drug Amphotericin B (d)



Microscope examination of VERO cells that incubated 24 h with St-g-P4ABA/PCL3 samples at 62.5µg/ml compared with untreated cells (control cells)

**Keywords** Corn starch · Hydrogels · Thermal stability · Swell ability · Degradation · Antimicrobial activity · Cytotoxicity

## Introduction

Hydrogels are superabsorbent polymers which are composed of lightly cross-linked networks of flexible polymer chains. They can absorb a large amount of water compared with general water absorbing materials in which the absorbed water is hardly removable even under certain pressure. Hydrophilic groups such as hydroxyl (OH) and carboxyl ( $-\text{COOH}$ ) on the polymer chains absorb and store water. If enough space exists within the hydrogel network, water molecules can become trapped and immobilized, filling the available free volume [1]. Because of their excellent characteristics, hydrogels have raised considerable interests and researches; they have been used in agriculture and horticulture, medicine for drug delivery system, artificial snow, sealing composites, shutoff water in oil wells, drilling fluid additives, controlling profile in water wells [2–5].

Although a variety of synthetic polymers such as polyacrylamide and polyvinyl alcohol copolymers and polymers of aspartic and acrylic acids have been employed for production of superabsorbent hydrogels [6–9], responding to the environmental concerns, many researches have been directed toward the use of biodegradable materials derived from natural sources such as starch, cellulose and CS, all of which are abundant in nature. But most of them do not have antibacterial activities to satisfy the need for the application. However, the antibacterial activity is one of the important performances of superabsorbent hydrogels in some fields, especially in hygiene and cosmetics field.

Starch is naturally present in a variety of botanical sources such as wheat, corn, yam, potato and tapioca. Starch is a biodegradable carbohydrate and is unique among all the carbohydrates because of its discrete particles called “granules”. Starch is not a thermoplastic polymer but can be processed after gelatinization. Starch characterized by biocompatibility, easy availability and hydrophilicity makes it a promising base material in preparation of superabsorbent hydrogels [10]. Although biodegradability of starch has made it popular in the scientific and industrial fields, raw starch has some defects which limit its industrial applications; this restriction dictates modifications. Starch has no antimicrobial activity, which limits its biomedical applications. Accordingly, physical and chemical modification is often necessary for functionality of natural starch. Modification changes the properties and behavior of the polymer, making it possible to get rid of unwanted characteristics while promoting desired ones [11]. Chemical modification of starch via graft copolymerization makes starch and modifier molecules bind together rather than existing simply as a physical mixture [12].

On the other hand, vinyl monomers, especially acrylic acid and its derivatives, are the main monomers in the synthetic absorbent polymers, due to their higher absorbent capacity [6]. Recently, many studies displayed that poly(acrylic acid) and poly (acrylamide) have an antimicrobial activity on many bacteria due to the presence of the hydrophilic amide ( $-\text{CONH}$ ) and carboxylic ( $\text{COOH}$ ) groups, which can inhibit the growth of microorganism. As published before, cold-plasma-grafted acrylic acid on a poly(ethylene) (PE) surface creates inhibition zones for *Staphylococcus aureus* [13] and radiation-grafted acrylic acid on

poly(ethylene terephthalate) surfaces reduced the number of colony-forming units of *Escherichia coli* [14]. Yang et al. [15] studied that the antimicrobial effect of polyacrylic acid against *Pseudomonas aeruginosa* increases with increasing mass of polyacrylic acid. Recently, Nahed et al. prepared grafted starch with 4-acrylamidobenzoic acid (ABA), a monomer that has the characteristic properties of both acrylic acid and acrylamide, which exhibited the higher antimicrobial activity [16]. Therefore, grafting of starch with vinyl monomers not only improves the absorbent capacity but also ameliorates its biological properties [17]. Compared to anionic or cationic graft copolymers, amphoteric absorbent polymers take much attention because they have potential salt-tolerant swelling character in addition to the higher antimicrobial properties.

It is well known that quaternary ammonium containing compounds constitutes a broad-spectrum chemical agent that can destroy or inhibit the growth of certain microorganisms. Among these chemical agents, poly(diallyldimethylammonium) chloride carries quaternary ammonium groups in its structure, which can interact electrostatically with the microbial cell wall leading to microbial membrane disruption [18].

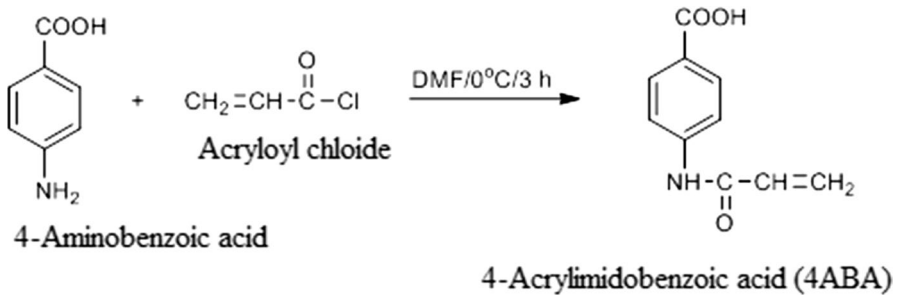
It seemed that no previous researches have been made to study the synthesis and the properties of amphoteric hydrogels resulted from grafted starch.

The present study aims to prepare a series of superabsorbent hydrogels having amphoteric character from gelatinized corn starch via grafting co-polymerization with *p*-acrylamidobenzoic acid (4ABA) and diallyl dimethyl ammonium chloride (CL) as cationic cross-linker in different concentrations (3%, 5%, 10% based on starch weight) to produce chemically cross-linked hydrogels designated as St-g-P4ABA/PCL3, St-g-P4ABA/PCL5 and St-g-P4ABA/PCL10, having amphoteric character with better chemical, physical and antimicrobial properties. The prepared hydrogels were evaluated to their antimicrobial activity against different kinds of bacteria and fungi. Their swelling behavior as well as the thermal stability was also studied. The structure of the prepared hydrogels was elucidated by FTIR, <sup>1</sup>H-NMR, SEM, XRD and TGA/DTGA.

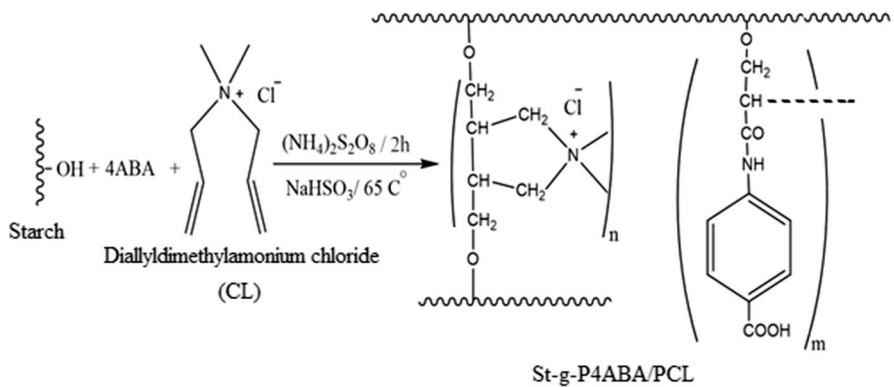
## Materials and experimental methods

### Materials

Starch was purchased from Nasr Chemical Co., Egypt (amylose content 25% and amylopectin content 75%). 4-Aminobenzoic acid and diallyldimethylammonium chloride were purchased from Loba Chemie. Solvents, reagents and all other chemicals were obtained from Sigma-Aldrich, Germany, and were used as received. The microorganisms used for both antibacterial and antifungal activities were provided by the Regional Center for Mycology and Biotechnology. 4-Acrylamidobenzoic acid monomer 4(ABA) was prepared from the reaction of acryloyl chloride with 4-aminobenzoic acid in DMF by the same method as reported previously. Whereas the calculated amount of acryloyl chloride (0.05 mol/L) was slowly added to a solution of 4-aminobenzoic acid (0.05 mol/L dissolved in DMF), the mixture was kept in ice



**Scheme 1** Schematic representation for preparation of 4ABA



**Scheme 2** Preparation of St-g-P4ABA/PCL hydrogel

bath on a magnetic stirrer for 3 h. After that the reaction mixture was poured on crushed ice to precipitate the crud product, which separated by filtration, washed several times with cold water and recrystallized from hot water, finally dried in oven at 60 °C for 8 h Scheme 1 [16].

## Experimental methods

### Preparation of cross-linked starch-g-P4ABA/PCL hydrogels

Scheme 2 shows the graft copolymerization of starch with both 4-acrylamidobenzoic acid (4ABA) (0.25 mol/L) and different amounts of diallyldimethylammonium chloride (CL) as follows: 1.0 g of dry corn starch in double-distilled water was heated at 85 °C for 30 min with continuous stirring to obtain a gelatinized corn starch, then the reaction temperature was decreased to 65 °C and a predetermined amounts of 4ABA (0.25 mol/L) and the cross-linker diallyldimethylammonium chloride (3, 5, 10% based on starch weight) were slowly added to the reaction mixture. The flask was placed in a water bath under nitrogen gas, and the grafting process was initiated by a dropwise addition of appropriate amount of

$(\text{NH}_4)_2\text{S}_2\text{O}_8/\text{NaHSO}_3$  ( $3 \times 10^{-2}$  mol/L), as a redox initiator. After 2 h, the resulted hydrogels were precipitated on cold methanol and kept on stirrer overnight for dewatering, then collected by filtration and washed with methanol several times and then dried in oven at  $65^\circ\text{C}$  for 8 h. Three hydrogels (based on the amount of the cross-linker added) were produced designated as St-g-P4ABA/PCL3, St-g-P4ABA/PCL5 and St-g-P4ABA/PCL10, respectively.

The grafting parameters: grafting percentage (%G), grafting efficiency (%GE) and homopolymer percentage (%H), which are summarized in Table 1, were determined as follows:

$$\%G = [(W_2 - W_0) / W_0] \times 100 \quad (1)$$

$$\%GE = [(W_1 - W_0) / (W_2 - W_0)] \times 100 \quad (2)$$

$$\%H = [(W_1 - W_2) / W_3] \times 100 \quad (3)$$

where  $W_0$  is the initial starch weight,  $W_1$  and  $W_2$  are the weight of grafted starch before and after Soxhlet, respectively, and  $W_3$  is the weight of the monomers charged.

## Characterization

### Antibacterial analysis

The antibacterial activity of St-P4ABA/PCL hydrogels was evaluated by agar well diffusion technique [19], against *Staphylococcus aureus* (ATCC 25,923) (*S. aureus*) and *Enterococcus faecalis* (ATCC 29,212) (*E. faecalis*) as gram-positive bacteria, and *Klebsiella pneumoniae* (ATCC BAA1705) (*K. pneumoniae*) as gram-negative bacteria. The activity was determined by measuring the diameters of inhibition zones (in mm). Each inhibition zone was measured three times by caliper to get an average value. *Ciprofloxacin* was used as an antibacterial standard drug.

Antifungal study was investigated by screening the tested samples separately in vitro against *Aspergillus fumigatus* (ATCC 46,645) (*A. fumigatus*), *Candida albicans* (ATCC 24,433) (*C. albicans*) fungi on sabouraud dextrose agar plates using the agar well diffusion technique. The culture of fungi was purified

**Table 1** Experimental vales of %G, %GE and %H of St-g-P4ABA/PCL hydrogels

Samples	%G	%GE	%H
St-g-P4ABA/PCL3	36	50	45
St-g-P4ABA/PCL5	41	60	40
St-g-P4ABA/PCL10	46	66	35

by the single-spore isolation method [20]. The activity was determined by measuring the inhibition zone diameter (mm). Each inhibition zone was performed three times for each fungus; *Amphotericin B* was used as an antifungal standard drug.

### Cytotoxicity evaluation using viability assay

For cytotoxicity assay, the cells (Normal VERO cell lines) were seeded in 96-well plate at a cell concentration of  $1 \times 10^4$  cells per well in 100  $\mu$ l of growth medium. Fresh medium containing different concentrations of the test sample was added after 24 h of seeding. Serial twofold dilutions of the tested chemical compound were added to confluent cell monolayers dispensed into 96-well, flat-bottomed microliter plates (Falcon, NJ, USA) using a multichannel pipette. The microliter plates were incubated at 37 °C in a humidified incubator with 5% CO<sub>2</sub> for a period of 24 h. Three wells were used for each concentration of the test sample. Control cells were incubated without test sample and with or without DMSO. The little percentage of DMSO present in the wells (maximal 0.1%) was found not to affect the experiment. After incubation of the cells, viable cells yield was determined by a colorimetric method (using 1% crystal violet stain: composed of 0.5% (w/v) crystal violet and 50% methanol then made up to volume with ddH<sub>2</sub>O and filtered through a Whatman No.1 filter paper).

All experiments were carried out in triplicate. The cell cytotoxic effect of each tested compound was calculated. The optical density was measured with the microplate reader (SunRise, TECAN, Inc, USA) to determine the number of viable cells, and the percentage of viability was calculated as  $[(OD_t/OD_c)] \times 100\%$  where OD<sub>t</sub> is the mean optical density of wells treated with the tested sample and OD<sub>c</sub> is the mean optical density of untreated cells. The relation between surviving cells and drug concentration is plotted to get the survival curve of each tumor cell line after treatment with the specified compound [21]. VERO cells (Mammalian cells from African Green Monkey Kidney) were obtained from VACSERA Tissue Culture Unit.

### Water and saline absorption measurements

Absorption behavior of the prepared hydrogels in both water and 0.9% saline solution was performed as a function of time as follows: known weight of the sample was soaked and kept undisturbed at room temperature in 20 ml liquid at different time intervals from 1 to 24 h till equilibrium swelling was reached, then removed from the immersion media, quickly wiped with filter paper to remove the droplets on its surface and reweighed. The swelling percent is calculated using the following equation:

$$\text{Swelling (\%)} = [(W_1 - W_0) / W_0] \times 100 \quad (4)$$

where  $W_0$  is the weight of the dry sample and  $W_1$  is the weight of the swollen sample. The measurements were taken in triplicate, and the estimated error was within 1% [16, 22].

## Degradation studies in different pH media

Degradation of the hydrogels was performed in vitro by placing the samples in different pH buffer solutions 4, 7 and 9 at room temperature 25 °C for different periods of time (1, 2, 4, 24, 48 and 96 h) using area/volume ratio = 0.1 cm<sup>-1</sup>. At each measurement, the samples were removed from the solution and then dried in the chamber at 40 °C and weighed after their weight stabilized. The degradation percentages (*D%*) were calculated based on the weight loss using the following equation [23]:

$$D\% = (W_0 - W_t) / W_0 \times 100 \quad (5)$$

where *W*<sub>0</sub> is the weight of dry sample, *W*<sub>*t*</sub> is the weight after the immersion time (*t*). Each degradation experiment was repeated three times, the average value was considered and the experimental error was within 1%.

## Swelling behavior of the St-g-P4ABA/PCL hydrogels in different pH media

Determination of the swelling ability of the hydrogels in different pH media: known weight of the dry hydrogel sample was submerged in a buffer solution of pH 4, 7 and 9 and held at room temperature as a function of time until swelling equilibrium was reached. The swelling percentage is calculated by using Eq. 4.

## Measurements

Fourier transform infrared spectroscopy (FTIR) was determined using Thermo FTIR Nicolet avatar 370CSI where the hydrogel samples were investigated as pellets with dry KBr from 400 to 4000 cm<sup>-1</sup> with a resolution of 4 cm<sup>-1</sup>.

Proton nuclear magnetic resonance (<sup>1</sup>H-NMR) spectra were investigated using a JEOL 270 MHz (Tokyo, Japan) spectrophotometer in dimethyl sulfoxide-d<sub>6</sub> (DMSO-d<sub>6</sub>) as a solvent, and the chemical shifts were recorded in ppm relative to TMS as an internal standard.

Surface morphology was studied by scanning electron microscopy (SEM) using Quanta FEG 250. The freeze-dried samples were loaded on the surface of an aluminum SEM specimen holder and sputter-coated with gold before photographed.

The X-ray diffraction patterns (XRD) of the native starch and starch hydrogels were determined at room temperature using Bruker's D-8 advanced wide-angle X-ray diffractometer. The X-ray source of 1.5406 Å wavelength was generated by a nickel-filtered CuKα radiation (40 kV, 30 mA). The dried samples were mounted on a sample holder and scanned in the reflection mode at an angle 2θ over a range from 4° to 70° at a speed of 2° min<sup>-1</sup>.

Thermogravimetric analysis (TGA/DTGA) was produced by Q500 TA under nitrogen (flow rate 50 ml/min) from room temperature to 600 °C at a rate of 10 °C/min.



## Results and discussion

Starch hydrogels were prepared via grafting copolymerization of gelatinized corn starch with 4-acrylamidobenzoic acid and diallyldimethylammonium chloride using  $(\text{NH}_4)_2\text{S}_2\text{O}_8/\text{NaHSO}_3$  as a redox initiator. The resulted hydrogels with their amphoteric character achieved better swell ability and higher antimicrobial activity than native starch. We expect these hydrogels promising materials in biomedical application and food industry.

### FTIR analysis

Figure 1 represents FTIR spectra of free starch and St-g-P4ABA/PCL3 hydrogel (as representative example for the prepared hydrogels). Spectrum of free starch exhibited characteristic bands at 3431 and 2928  $\text{cm}^{-1}$  related to stretching vibrations of OH and  $\text{CH}_2$  groups, respectively, peak at 1640  $\text{cm}^{-1}$  of lower intensity attributed to the contaminated proteins and fat. The bending vibration of the  $\text{CH}_2$  groups appeared at 1428  $\text{cm}^{-1}$ , and the peaks at 1157, 1082 and 1017  $\text{cm}^{-1}$  are corresponding to C–O–C, C–C and C–OH, respectively, and the peak at 857  $\text{cm}^{-1}$  is related to glucopyranose ring [16, 24]. Spectrum of St-g-P4ABA/PCL3 hydrogel showed in addition to starch characteristic peaks another new peak at 1695  $\text{cm}^{-1}$  corresponding to  $-\text{COOH}$  group and two peaks at 1606, 1536  $\text{cm}^{-1}$  attributed to  $\text{C}=\text{C}$  of benzene ring of 4ABA; moreover, the peak at 767  $\text{cm}^{-1}$  is attributed to the para-substituted benzene ring. It also showed characteristic band at 1335  $\text{cm}^{-1}$  related to the free methyl groups of the cross-linker diallyldimethylammonium chloride, the significant increase in the peaks intensity at 2926

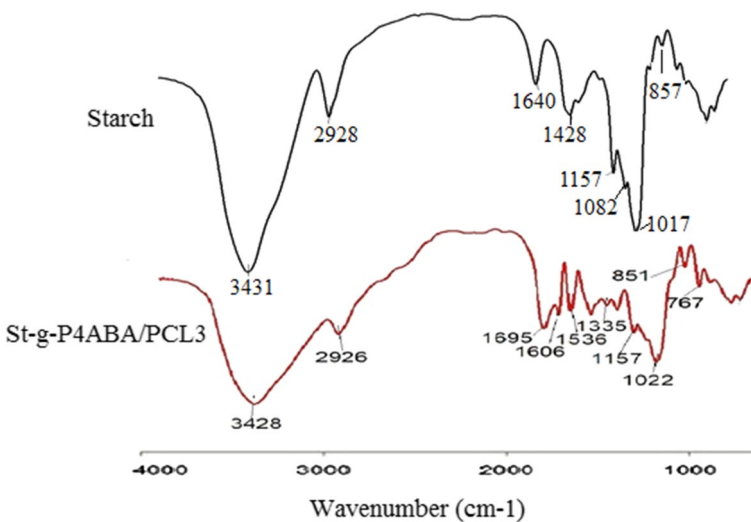


Fig. 1 FTIR spectra of starch and St-g-P4ABA/PCL3

and  $1022\text{ cm}^{-1}$  is due to the additional  $\text{CH}_2$  and  $\text{C-N}$  groups of the cross-linker molecules. These data are adequate to confirm the formation of starch hydrogel

### **$^1\text{H-NMR}$ spectra of starch and St-g-P4ABA/PCL hydrogel**

$^1\text{H-NMR}$  analysis gives additional confirmation to the structure of the prepared hydrogels. Spectrum of starch was given for comparison, which exhibited the common polysaccharide signals designated as follows: signal at  $\delta=5.323$  to  $5.395\text{ ppm}$  is corresponded to the carbon1 protons ( $\text{CH}_1$ ), broad signal at  $\delta=3.587$  to  $3.658\text{ ppm}$  is attributed to the protons of carbon 2, 3 and 4 ( $\text{CH-2}$ , 3, 4). The singlet at  $\delta=4.491\text{ ppm}$  and  $5.023\text{ ppm}$  is related to the protons of carbon 6 ( $\text{CH-6}$ ) and 5 ( $\text{CH-5}$ ), respectively [16]. On the other hand, spectrum of St-g-P4ABA/PCL hydrogel displayed the following signals: high-intensity signal at  $\delta=2.501$  related to protons on the carbon atoms 12, 13 ( $\text{CH-12}$ , 13), broad and high-intensity signal at  $\delta=3.528\text{ ppm}$  is corresponded to the protons on carbon 2, 3, 4, 9, 10 and quaternary ammonium protons ( $\text{N}^+(\text{CH}_3)_2$ ). The singlet at  $\delta=4.345\text{ ppm}$  is related to the carbon 6, 11, 14 protons ( $\text{CH-6}$ , 11, 14), while the signal at  $\delta=4.859\text{ ppm}$  is due to the protons of carbons 5 and 7 ( $\text{CH-5}$ , 7), the doublet at  $5.370$  and  $5.448$  are related to the protons on carbons 1 and 8 ( $\text{CH-1}$ , 8). It also showed a multiplet signal expanded from  $7.527$  to  $7.701$  corresponded to the phenyl protons (4H, para-substituted benzene ring), and signal at  $\delta=10.089$  and  $11.740\text{ ppm}$  is assigned to the  $\text{NH}$  and  $-\text{COOH}$  protons, respectively. The aforementioned data confirm the successful formation of the starch hydrogel as shown in Supplementary Figure (Suppl. 1).

### **X-ray diffraction study**

Figure 2 shows the X-ray pattern of St-g-P4ABA/PCL3 hydrogel (as a representative example for the prepared hydrogels) together with the patterns of native starch and gelatinized starch for comparison. From the patterns, we notice that neat starch has crystalline structure indicated by the presence of the four prominent intensity peaks at  $2\theta=15.2^\circ$   $16.9^\circ$   $18.1^\circ$  and  $23.2^\circ$ . Gelatinized starch exhibited a lower crystallinity than dry starch as detected from the disappearance of the diffraction peaks at  $15.2^\circ$ ,  $16.9^\circ$  and  $18.1^\circ$ , in addition to the increase in the broadness of the peak at  $23.2^\circ$ , and appearance of a new broad peak at  $17.4^\circ$  [16, 25]. The prepared St-g-P4ABA/PCL3 hydrogel showed the lower crystalline structure than gelatinized starch, since it exhibited only one broad peak around  $2\theta=20^\circ$  with the disappearance of the other crystalline peaks. It seems that grafting process with both 4ABA and diallyldimethylammonium chloride resulted in a significant decrease in the inter- and intramolecular hydrogen bonds, which is replaced by both 4ABA and the long-chain cross-linker molecules, leading to more open structure. These results are good evidence to the formation of St-g-4PABA/PCL hydrogels.

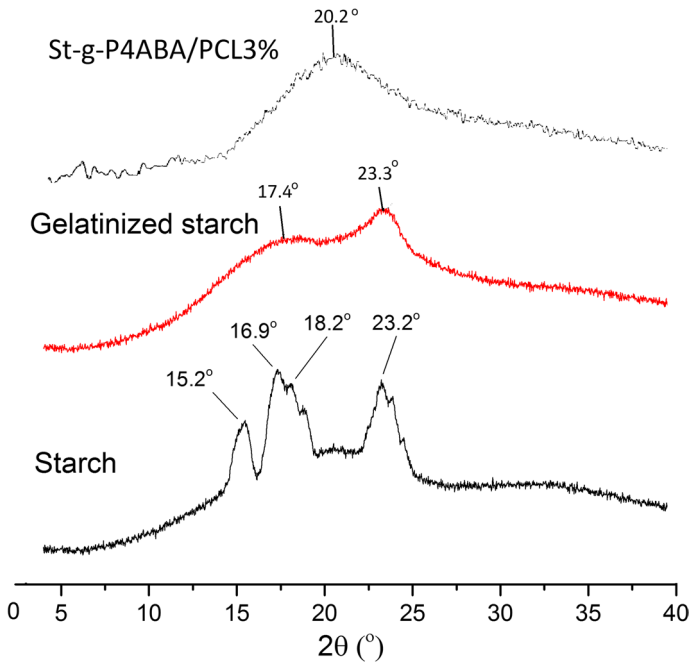


Fig. 2 X-ray diffraction patterns of starch, gelatinized starch and St-g-P4ABA/PCL3 hydrogel

### Thermogravimetric analysis

Figure 3 illustrates both TGA and DTGA of native starch and St-g-P4ABA/PCL hydrogels. From TGA and DTGA curves, native starch exhibited two stages of degradation. Stage I was extended from 35 to 128 °C due to releasing of absorbed water with mass loss of 7.8% of the original weight. Stage II was the main stage,

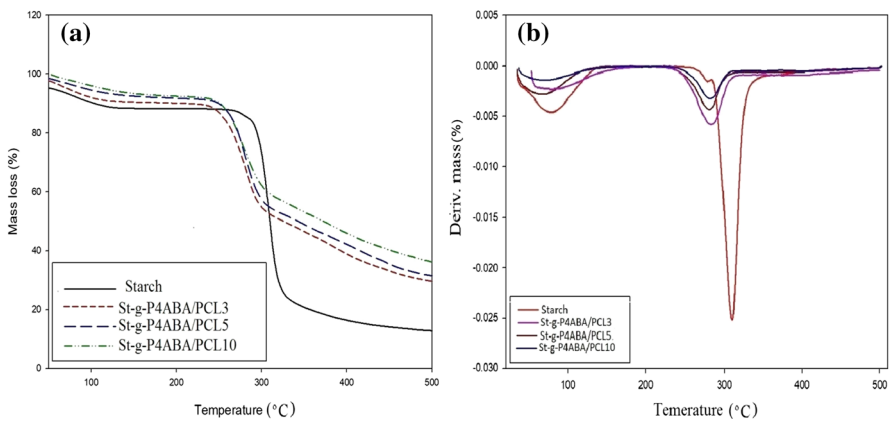


Fig. 3 TGA and DTGA patterns of starch, St-g-P4ABA/PCL hydrogels

extended from 235 °C to 500 °C due to degradation of starch backbone and removal of the carbonaceous products with mass loss of 77% and residual mass of 16%, and the maximum degradation was observed at 309 °C [16]. The thermogram of St-g-P4ABA/PCL hydrogels showed three degradation stages: the first one extended from 30 °C to 120 °C due to evaporation of free and bound water from the hydrogel matrix. Stage II and stage III constitute the actual polymer degradation; in stage II, the polymer started the decomposition over a broad range of temperature from 250 °C to 389 °C, which might be due to the degradation of the PCL-grafted chains and dissociation of quaternary ammonium salt [26]. The maximum rate of weight loss was found to be at about 283 °C for the all derivatives as indicated from the DTGA thermograms. In stage III, the breakage of C–C and C–O bonds of P4ABA-grafted chains, removal of CO<sub>2</sub>, NH<sub>3</sub> and the carbonaceous components took place at a temperature ranging from 389 °C to 501 °C, the residual masses at the end of this stage were 35%, 38% and 40% of St-g-P4ABA/PCL3, St-g-P4ABA/PCL5 and St-g-P4ABA/PCL10, respectively, while 16% of native starch. The increase in the initial decomposition temperature and in the residual masses of St-g-P4ABA/PCL hydrogels than native starch indicates the thermal stabilizing effect of the grafted molecules on corn starch, which increased with increasing graft percent.

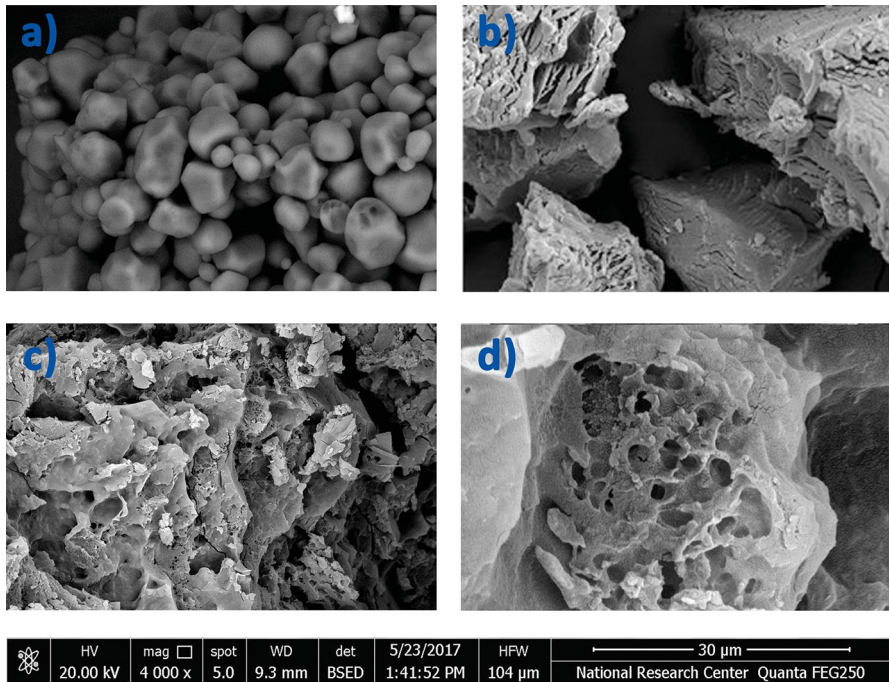
### Scanning electron microscopy observation

Figure 4a–e shows the changes in the morphological structure of corn starch after grafting process by using scan electron microscopy. Compared to the smooth surface of granular starch (a), gelatinized starch has a rough surface and opened structure (b) [16], while the surface morphology of starch hydrogels exhibited porous structure and the pores homogeneously distributed through the hydrogel matrix (c, d). The amount of pores increased and became more uniform with increasing cross-linking density from St-g-P4ABA/PCL3 to St-g-P4ABA/PCL10. Additional information about the composition of the hydrogels was given from EDX (Suppl. 2).

### Swelling behavior of the St-g-P4ABA/ PCL hydrogels in water and 9% saline solution

The swelling behavior of any polymer network depends upon the nature of the polymer, polymer solvent compatibility and degree of cross-linking. However, in case of ionic networks, swelling behavior depends mainly on the ionic interaction [27, 28].

The swelling behavior of the St-g-P4ABA/ PCL hydrogels in both water and 0.9% saline solution as a function of time revealed that compared with free starch all the prepared hydrogels exhibited higher swell ability in both water and 9% saline solution, whereas the swelling behavior depends mainly on three factors: (1) the electrostatic repulsion interaction between the similar charges created on the hydrogel matrix which resulted in osmotic imbalances leading to much diffusion of the liquids inside the hydrogels, (2) the porous structure of the hydrogel which can absorb and retain large amount of solvents for long time, (3) the large distance between the neighboring chains which allow the hydrogels to absorb much liquid.



**Fig. 4** SEM images of **a** free starch, **b** gelatinized starch, **c** St-g-P4ABA/PCL10, **d** St-g-P4ABA/PCL3 hydrogels at magnification of 4000x

Moreover, the swell ability data showed that the swelling percent of starch hydrogels in 9% saline solution is greater than in water; this might be due to the greater electrostatic repulsion interaction between the quaternary nitrogen ( $N^+$ ) of the cross-linker and the  $Na^+$  ions of saline solution which increased the ions mobility and leading to much diffusion of the liquid inside the hydrogel matrix. It seemed that the swelling % increased with increasing of %G from 36 to 46 as illustrated in Table 2, whereas St-g-P4ABA/ PCL10 hydrogel with %G 46 exhibited higher swelling percent in saline solution and water. Figure 5a, b depicts the kinetic correlation between swell ability % and time in water and saline solution, which illustrated that as the time increases the swelling ability readily increases reaching the equilibrium after 240 min, whereas the swell ability slightly increased.

**Table 2** Absorption behavior of starch and St-g-P4ABA/ PCL hydrogels in water and 9% saline solution

Sample	%G	Water uptake% (g/g sample)	Saline uptake% (g/g sample)
Starch	0	1406	1330
St-g-P4ABA/ PCL3	36	2350	2528
St-g-P4ABA/ PCL5	41	2500	2650
St-g-P4ABA/ PCL10	46	2686	2796

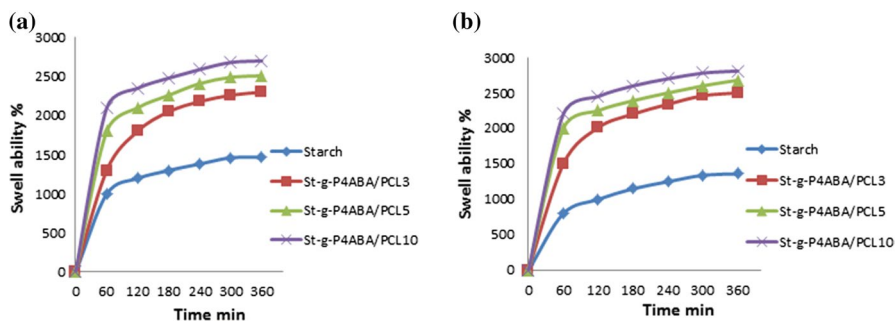


**Fig. 5** Swell ability behavior of starch and St-g-P4ABA/PCL hydrogels **a** in water and **b** in saline solution

### Degradation behavior of St-g-P4ABA/PCL at different pH media

Table 3 illustrates the degrading behavior of the St-g-P4ABA/PCL5 (as a representative example) in different pH buffer solutions of 4, 7 and 9 at room temperature 25 °C at various time intervals (1, 2, 3, 4, 24, 48 and 96). The data showed that the hydrogel exhibited significant stability at all pH media, especially at pH=7 the hydrogel was fully stable, slight degradation was observed after 96 h and the *D*% was about 5%. At pH=4, the degradation percentage of the hydrogel after 1 h was 9% and steadily increased to 21% after 96 h, while at pH=9 The *D*% was 7% after 1 h increased with time to reach 32% after 96 h [23].

### Swelling behavior of the St-g-P4ABA/PCL hydrogels at different pH media

Swelling of St-g-P4ABA/PCL hydrogels at room temperature in different pH buffer solutions (4, 7 and 9) over different periods of time revealed that swell ability of the hydrogels increased rapidly with time up to 240 min and then leveled off. They exhibited higher degree of swell ability in both acidic and basic media than in neutral medium, whereas the St-g-P4ABA/PCL hydrogels are characterized by amphoteric character, having free positively charged species  $N^+(CH_3)_2$  and free  $-COOH$  groups, Thus, in an acidic medium (pH=4) the higher swell ability resulted from the repulsive interaction between the  $N^+(CH_3)_2$  groups which resulted in different osmotic pressure inside the hydrogel network and the liquid outside, leading to much diffusion into the hydrogel matrix, while in basic medium (pH=9) the

**Table 3** Degradation behavior of St-g-P4ABA/PCL hydrogels at different pH media

pH	Samples	1 h	2 h	3 h	4 h	24 h	48 h	96 h
7	St-g-P4ABA/PCL5	0	0	0	0	2	3	5
4	St-g-P4ABA/PCL5	9	10	11	12	13	17	21
9	St-g-P4ABA/PCL5	7	9	12	13	14	18	23

–COOH groups converted to  $\text{–COO}^-$  anion and the electrostatic repulsion interaction between the similar negatively charged ions resulted in an increase in the ionic mobility inside the hydrogel network, leading to the higher swelling ability [29, 30]. Swelling ability in neutral medium located between them as a result of the bonded water molecules to the hydrogel functional groups. It is worth mentioning that the degree of swell ability increases as the graft percentage increases from St-g-P4ABA/PCL3 to St-g-P4ABA/PCL10 as a result of increase in the free charged species on the hydrogel back bone. The correlation between the swelling % and the pH is depicted in Fig. 6.

## Antimicrobial study

### Antibacterial assay

Antibacterial activity of starch and starch hydrogels St-g-P4ABA/PCL against *S. aureus*, *E. faecalis* as gram-positive bacteria and *K. pneumoniae* as gram-negative bacteria was done by measuring the zones of inhibition using the agar well diffusion technique; the results of ciprofloxacin as a standard reference drug were also given for comparison. The antimicrobial data of St-g-P4ABA that reported on the same strains in our previously published work were also given for comparison [16]. From the inhibition zone data, we observed that starch had

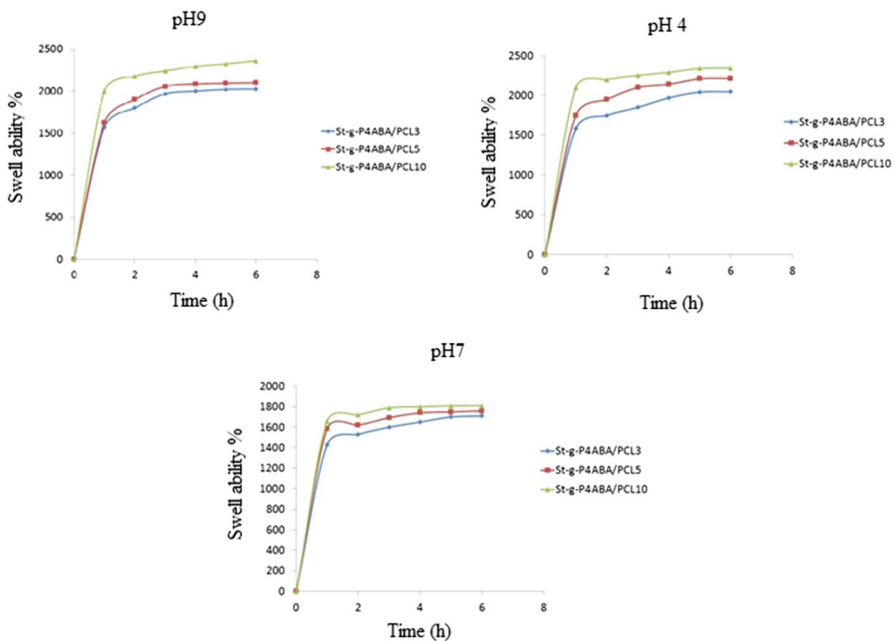


**Fig. 6** Swell ability behavior of St-g-P4ABA/PCL 3, St-g-P4ABA/PCL 5 and St-g-P4ABA/PCL 10 in different pH media



no inhibitory effect on bacterial growth as reported before [16, 31], while St-g-P4ABA exhibited significantly higher antibacterial activity toward the tested pathogens, especially against gram-negative bacteria strains it displayed inhibition zone diameters ranged from  $14.1 \pm 2.1$  to  $17.9 \pm 1.5$  mm. The antibacterial activity of grafted starch was enhanced by incorporation of the cationic cross-linker diallyldimethylammonium chloride. As shown from the inhibition zone data, the prepared St-g-P4ABA/PCL hydrogels exhibited higher potency in suppressing the bacterial growth than uncross-linking sample St-g-P4ABA as indicated from their higher inhibition zone diameters which ranged from  $15.3 \pm 1.2$  to  $21.4 \pm 0.58$  mm. The increment of the antibacterial activity of the hydrogels might be due to the incorporated quaternary ammonium groups, which increases the electrostatic interaction with the phosphate groups of the bacterial cell membranes [18, 32] causing disintegration of the cell membrane. Moreover, the efficiency of the hydrogels on inhibition bacterial growth increases with increasing the cross-linking density. Thus, the St-g-P4ABA/PCL10 hydrogel exhibited higher inhibition zone diameters than St-g-P4ABA/PCL3 hydrogel, especially on gram-negative bacteria than gram-positive bacteria. The results revealed that the highest antibacterial hydrogel St-g-P4ABA/PCL10 showed inhibition zones of  $21.4 \pm 2.1$ ,  $20.4 \pm 1.5$  and  $18.1 \pm 1.5$  mm against *K. pneumoniae*, *E. faecalis* and *S. aureus*, respectively, while the lowest antibacterial hydrogel St-g-P4ABA/PCL3 exhibited inhibition zones of  $18.1 \pm 0.58$ ,  $17.4 \pm 1.2$  and  $15.3 \pm 1.5$  mm against the same strains, respectively, corresponding to inhibition zones of  $23.4 \pm 1.2$ ,  $27.4 \pm 0.72$  and  $23.4 \pm 0.63$  mm of the reference drug *Ciprofloxacin* against the tested microorganisms, respectively. These results were supported by the lower MIC values of the hydrogels against the tested microorganisms; thus, their measured MICs ranging from 1.95 to 3.9  $\mu\text{g/ml}$  are very close to the MIC values recorded by the reference drug ciprofloxacin (in the range of 0.49–0.98  $\mu\text{g/ml}$ ) as given in Table 3. The observed higher antibacterial activity of the prepared hydrogels might result from: (1) the hydrophilic nature of the hydrogels, which facilitate the contact with the bacterial cell membrane; (2) the amphoteric character of the hydrogel increases the ionic interaction with the charged cell membranes and thus alters their function, leading to leakage of the cellular components, and consequently inhibits the growth of the microorganisms; (3) the polar groups (OH, COOH, NH,  $\text{R}_2\text{N}^+$ ) in the hydrogel structure allow better chelation with the essential metals of the nutrient responsible for bacterial growth. These factors together enhance the suppression activity of starch hydrogels on microbial growth [16, 31]. The inhibition zone indices are depicted in Fig. 7. It is worth mentioning that the different antimicrobial efficiencies of the hydrogels on both types of bacteria might be due to the different cell wall structures since gram-positive bacteria cell membrane is composed of peptidoglycan layer and teichoic acid with porous structure, while gram-negative is composed of thin layer of peptidoglycan and an outer membrane of phospholipids, phosphoprotein and polysaccharide.

The agar plates that illustrated the inhibition zone diameters (mm) of starch, St-g-P4ABA/PCL3 and St-g-P4ABA/PCL10 together with the antibacterial reference drug ciprofloxacin against the tested bacteria (*S. aureus*, *E. faecalis* as gram-positive bacteria and *K. pneumoniae* as gram-negative bacteria) are shown in Fig. 8.



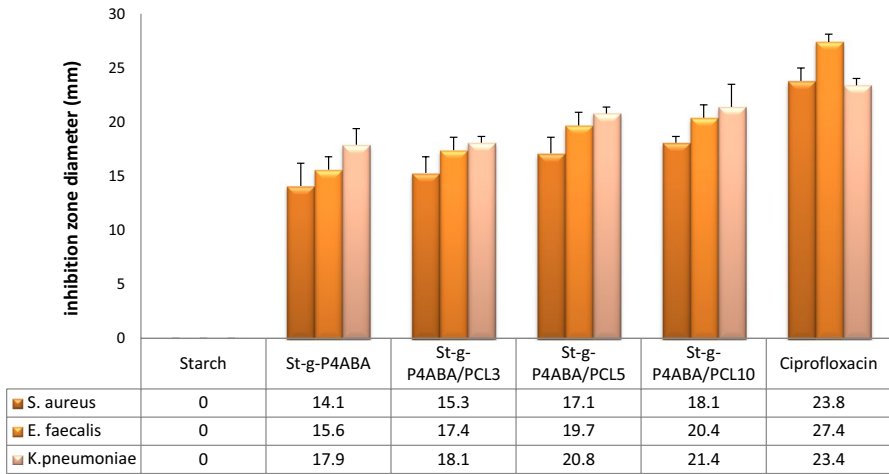


**Fig. 7** Inhibition zone diameter of starch, St-g-P4ABA and St-g-P4ABA/PCL hydrogels against *S. aureus*, *E. faecalis* and *K. pneumoniae*

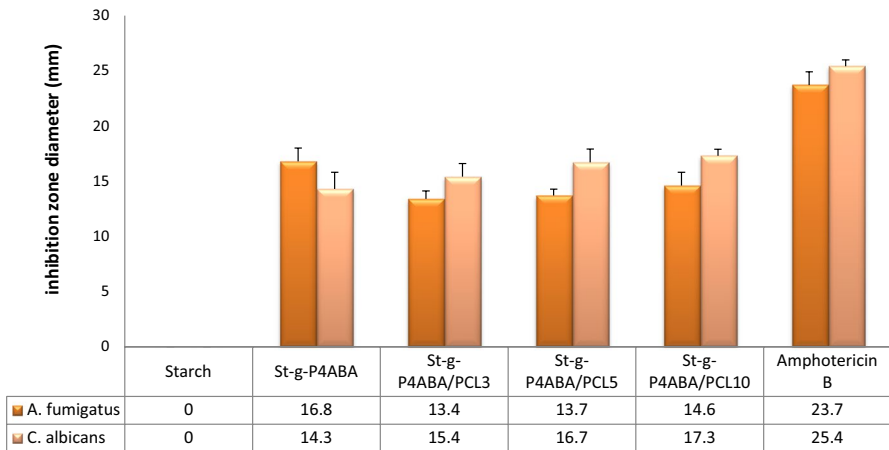


**Fig. 8** Inhibition zone diameters of starch, St-g-P4ABA, St-g-P4ABA/PCL hydrogels and amphotericin B against *A. fumigatus* and *C. albicans*

### Antifungal activity assay

Starch and St-g-P4ABA/PCL hydrogels were in vitro screened for antifungal activity against *A. fumigatus* and *C. albicans* using amphotericin B as a reference standard drug, the antimicrobial data of the uncross-linked St-P4ABA sample on the same strains that reported in our previous published work were given for comparison [16]. The investigation preceded using the agar well diffusion method by measuring the inhibition zone diameters. The results showed that starch had no inhibition activity toward fungi growth, while St-g-P4ABA showed suppression in fungi

growth as observed from the higher inhibition zone diameters against the tested fungi, whereas St-g-P4ABA exhibited inhibition zones of  $16.8 \pm 1.2$  mm against *A. fumigatus* and  $14.3 \pm 1.5$  mm against *C. albicans*. On the other hand, the antifungal investigation of the prepared starch hydrogels against the same microorganisms revealed that all starch hydrogels displayed higher efficiency in inhibiting the growth of fungi. It seemed that the antifungal activity increased with increasing the cross-linking density, whereas St-g-P4ABA/PCL3 exhibited lower antifungal activity than St-g-P4ABA/PCL10, while St-g-P4ABA/PCL5 lie in between them. The data showed that the St-g-P4Aba/PCL hydrogels displayed inhibition zones ranging from  $13.4 \pm 0.72$  to  $14.6 \pm 0.58$  mm against *A. fumigatus* and ranging from  $15.4 \pm 1.2$  to  $17.3 \pm 1.2$  mm against *C. albicans* corresponding to inhibition zones of  $23.7 \pm 1.2$  and  $25.4 \pm 0.58$  mm for the reference drug amphotericin B against the same strain, respectively. The results were supported from the lower MIC values of the tested hydrogels. They exhibited MICs ranged from 1.95 to 3.9  $\mu\text{g/ml}$  against the tested fungi close to those obtained for the reference drug amphotericin B (MIC values ranged from 0.49 to 0.98  $\mu\text{g/ml}$ ). The observed higher antifungal activity of the hydrogels might result from their higher hydrophilicity, and the presence of a large number of ionic species facilitates the diffusion of the hydrogel active ingredients inside the hyphae of fungi disturbing the enzyme activity responsible for fungal growth. Further, the carboxylic groups in the hydrogel matrix can bind physicochemically to ergosterol in fungal membrane leading to loss of cell permeability, leakage of vital cytoplasmic components and suppression of fungal growth [33, 34]. In contrast to St-P4ABA, all hydrogels displayed better antifungal activity against *C. albicans* than *A. fumigatus*, which may be due to the different membrane composition of both fungi; the results are depicted in Fig. 9.

The agar plates which illustrated the inhibition zone diameters of free starch, the hydrogels and the reference drug amphotericin B against *A. fumigatus* and *C. albicans* are given in Fig. 9 and Table 4

### Evaluation of cytotoxicity St-g-P4ABA/PCL hydrogels on (VERO) cell line

Cytotoxicity is an important test to choose the biomaterials used in biomedical application; on this respect, the biomaterials must have lower cytotoxicity on normal human cells. Herein, the cytotoxicity of the new prepared St-g-P4ABA/PCL3 hydrogel as a biomaterial was studied against (normal VERO cells lines) using different sample concentrations from 0 to 500  $\mu\text{g/ml}$  by colorimetric method; the results revealed that starch hydrogels exhibited no inhibition to the viability of the normal VERO cells at concentration lower than 15.6  $\mu\text{g/ml}$  since the viability was 100%. The viability of the intact VERO cells gradually decreased with increasing sample concentrations from 15.6 to 500  $\mu\text{g/ml}$  as illustrated from Fig. 10a.

The low cytotoxicity of starch hydrogel was further supported from screening the morphological changes that occurred on the Vero cells after incubation with tested hydrogel.

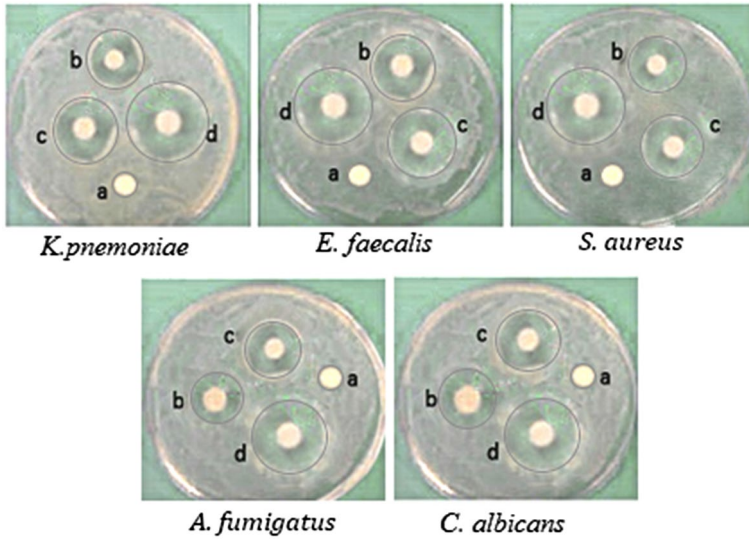


**Fig. 9** Normal photographs for the antimicrobial behavior of free starch (a), St-g-P4ABA/PCL3 (b), St-g-P4ABA/PCL10 (c) against *E. faecalis* and *S. aureus* as gram-positive bacteria against *K. pneumoniae* as gram-negative bacteria in comparison with the antibacterial standard drug ciprofloxacin (d) and against *A. fumigatus* and *C. albicans* as fungi in comparison with the antifungal standard drug Amphotericin B (d)

**Table 4** Minimum inhibitory concentration indices of the St-g-P4ABA/PCL hydrogels against *K. pneumoniae*, *E. faecalis*, *S. aureus*, *C. albicans* and *A. fumigatus*

Samples	Minimum inhibitory concentration (MIC) µg/ml				
	Tested bacteria			Tested fungi	
	<i>K. pneumoniae</i>	<i>E. faecalis</i>	<i>S. aureus</i>	<i>C. albicans</i>	<i>A. fumigatus</i>
St-g-P4ABA/PCL3	1.95	3.9	1.95	1.95	3.9
St-g-P4ABA/PCL5	1.95	3.9	1.95	1.95	3.9
St-g-P4ABA/PCL10	1.95	3.9	1.95	1.95	3.9
<i>ciprofloxacin</i>	0.98	0.49	0.49	–	–
<i>Amphotericin B</i>	–	–	–	0.49	0.98

by an inverted microscope. The microscopic examination of VERO cells incubated for 24 h with different concentrations of hydrogel compared to untreated cells (control cells) is shown in Fig. 10b.

However, according to the results summarized in Table 3, all St-g-P4ABA/PCL hydrogels exhibited higher antibacterial and antifungal activity against the tested microorganisms, and their minimum inhibitory concentration (MIC) was ranging from 1.95 to 3.9 µg/ml, which is lower than 15.6 µg/ml, the lowest concentration that resulted in cytotoxicity for the intact VERO cells; thus, the prepared

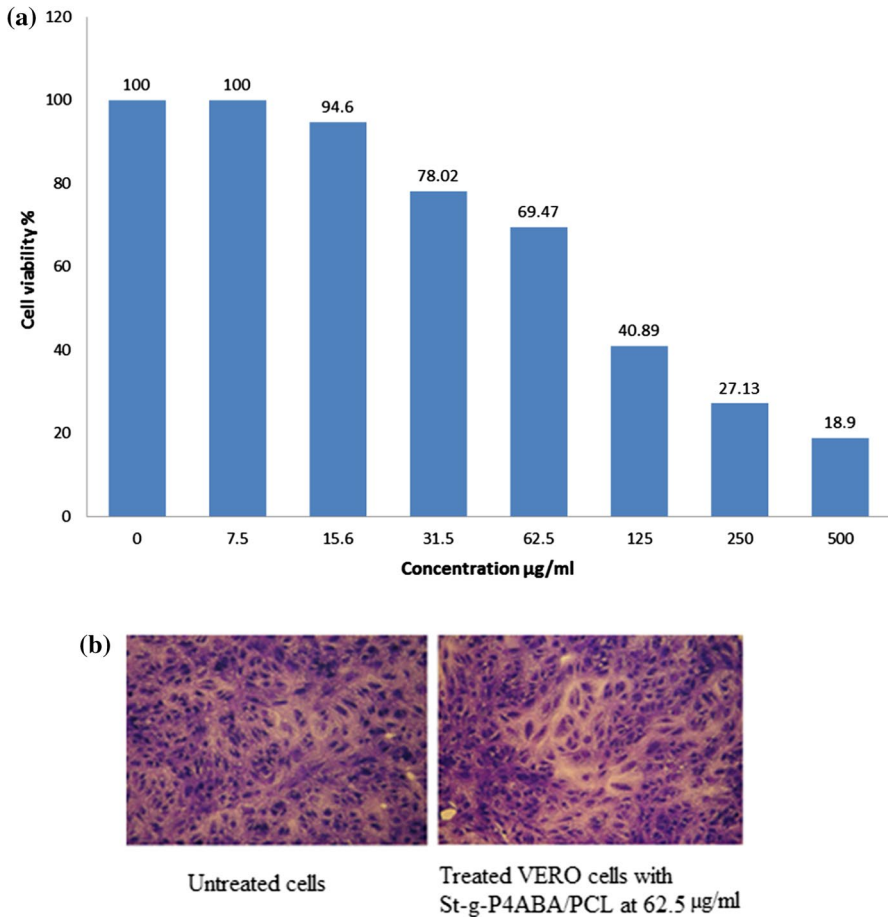


**Fig. 10** **a** Cell viability percentage of different concentrations of St-g-P4ABA/PCL3 hydrogel after 24-h incubation with VERO cell lines and **b** microscope examination of VERO cells that incubated 24 h with starch hydrogel samples at 62.5  $\mu\text{g/ml}$  compared with untreated cells (control cells)

St-g-P4ABA/PCL hydrogels can be used as antimicrobial agents in medicine for pharmaceutical applications without dangerous effect on the intact cells.

## Conclusions

Novel hydrogels based on biodegradable polymer having amphoteric character were successfully synthesized from corn starch grafted with p-acrylamidobenzoic acid and diallyldimethylammonium chloride as potent salt-tolerant hydrogels and effective antimicrobial agents. The structure of them was proven by physical and chemical tools. They displayed higher thermal stability at elevated temperature and higher residual mass than native starch. Swelling behavior of the new hydrogels in

water and 9% saline solution at different time intervals revealed that the swelling rate increased with increasing time and leveled off after 240 min. The swell ability measurements showed that all hydrogels exhibited significantly higher swell ability in saline solution and in acidic and basic buffer solutions rather than in neutral solution, which might be due to their amphoteric character and the presence of mobile ions inside their matrix. The swelling degree clearly increased with increasing cross-linking density. Degradation studies at pH buffer solution 4, 7 and 9 showed significant stability of the hydrogels up to 24 h, especially at pH=7; there is no degradation which was observed up to 48 h. The hydrogels displayed antimicrobial potency against gram-positive and gram-negative bacteria and fungi without cytotoxic effect on the normal human cells as shown from the cytotoxicity investigation, especially at low concentration. We can recommend these hydrogels as good salt-tolerant and active antimicrobial agents in industrial and biomedical applications without dangerous effect on intact human cells.

### Compliance with ethical standard

**Conflict of interest** The authors declare that they have no conflict of interest.

### References

1. Pal K, Banthia A, Majumdar D (2006) Preparation of transparent starch based hydrogel membrane with potential application as wound dressing. *Trends Biomater Artif Organs* 20(1):59–67
2. Deng Y et al (2010) Multifunctional mesoporous composite microspheres with well-designed nano-structure: a highly integrated catalyst system. *J Am Chem Soc* 132(24):8466–8473
3. Zhong H et al (2008) Controlled synthesis and optical properties of colloidal ternary chalcogenide CuInS<sub>2</sub> nanocrystals. *Chem Mater* 20(20):6434–6443
4. Zhou M et al (2012) Synthesis and characterization of salt resistance hydrogel microspheres by inverse suspension polymerization. *E-Polymers* 12(1):1–11
5. Wan T et al (2006) Preparation of a kaolinite–poly (acrylic acid acrylamide) water superabsorbent by photopolymerization. *J Appl Polym Sci* 102(3):2875–2881
6. Erizal E (2012) Synthesis of poly (acrylamide-co-acrylic acid)-starch based superabsorbent hydrogels by gamma radiation: study its swelling behavior. *Indones J Chem* 12(2):113–118
7. Mofidfar M, Kim ES, Larkin EL, Long L, Jennings WD (2019) Antimicrobial activity of silver containing crosslinked poly(acrylic acid) fibers. *Micromachines (Basel)* 10:829–841
8. Meimoun J et al (2018) Modification of starch by graft copolymerization. *Starch-Stärke* 70(1–2):1600351
9. Djordjevic S, Nikolic L, Kovacevic S, Miljkovic M, Djordjevic D (2013) Graft copolymerization of acrylic acid onto hydrolyzed potato starch using various initiators. *Chem Eng* 57(1–2):55–61
10. Nairretti D, Mironescu M, Tita O (2014) Antimicrobial activity of active biodegradable starch films on pathogenic microorganisms. *Ann Rom Soc Cell Biol* 19(1):75–80
11. Zhang B, Zhou Y (2008) Synthesis and characterization of graft copolymers of ethyl acrylate/acrylamide mixtures onto starch. *Polym Compos* 29(5):506–510
12. Cankaya N (2018) Modification of starch: structural and antimicrobial properties. *IJCCE* 3:31–35
13. Popelka A et al (2012) A new route for chitosan immobilization onto polyethylene surface. *Carbohydr Polym* 90:1501–1508
14. Ping X, Wang M, Xuewu G (2011) Surface modification of poly(ethylene terephthalate) (PET) film by gamma-ray induced grafting of poly(acrylic acid) and its application in antibacterial hybrid film. *Radiat Phys Chem* 80:567–572

15. Yang JM, Lin HT, Wu TH, Chen CC (2003) Wettability and antibacterial assessment of chitosan containing radiation-induced graft nonwoven fabric of polypropylene-g-acrylic acid. *J Appl Polym Sci* 90:1331–1336
16. El-Ghany NAA et al (2019) Antimicrobial and swelling behaviors of novel biodegradable corn starch grafted/poly (4-acrylamidobenzoic acid) copolymers. *Int J Biol Macromol* 134:912–920
17. Sabaa MW, Magid EA, Mohamed RR (2017) Maize Starch-g-Poly (itaconic acid) and its application in sewage water treatment and as antimicrobial agent. *Sci Rev Chem Commun* 7(1):1–17
18. Sanches LM et al (2015) The antimicrobial activity of free and immobilized poly (diallyldimethylammonium) chloride in nanoparticles of poly (methylmethacrylate). *J Nanobiotechnol* 13:58
19. Rahman A, Choudhary MI, Thompson WJ (2001) Preparation and antimicrobial activity of some carboxymethyl chitosan acyl thiourea derivatives. *Pestic Res J* 16:2024–2027
20. Rathore H, Mittal S, Kumar S (2000) Synthesis, characterization and antifungal activities of 3d transition metal complexes of 1-acetyl piperazinyldithiocarbamate, M (acpdtc) 2. *Pestic Res J* 12:103–107
21. Mosmann T (1983) Rapid colorimetric assay for cellular growth and survival: application to proliferation and cytotoxicity assays. *J Immunol Methods* 65:55–63
22. Mohamed NA, Abd El-Ghany NA, Fahmy MM (2016) Novel antimicrobial superporous cross linked chitosan/pyromellitimide benzoyl thiourea hydrogels. *Int J Biol Macromol* 82:589–598
23. Mohamed RR, Abu Elella MH, Sabaa MW (2015) Synthesis characterization and applications of N-quaternized chitosan/poly(vinyl alcohol) hydrogels. *Int J Biol Macromol* 80:149–161
24. Kizil R, Irudayaraj J, Seetharaman K (2002) Characterization of irradiated starches by using FT-Raman and FTIR spectroscopy. *J Agric Food Chem* 50(14):3912–3918
25. Utrilla-Coello RG et al (2014) Acid hydrolysis of native corn starch: morphology, crystallinity, rheological and thermal properties. *Carbohydr Polym* 103:596–602
26. Francis S, Varshney L, Sabharwal S (2007) Thermal degradation behavior of radiation synthesized polydiallyldimethylammonium chloride. *Eur Polymer J* 43:2525–2531
27. Ganji F, Farahani SV, Farahani EV (2010) Theoretical description of hydrogel swelling: a review. *Eur Polym J* 19(5):375–398
28. Ahmed EM (2015) Hydrogel: Preparation, characterization, and applications: a review. *JAR* 6(2):105–121
29. Chang C, He M, Zhou J, Zhang L (2011) Swelling Behaviors of pH- and salt-responsive cellulose-based hydrogels. *Macromolecules* 44:1642–1648
30. Al-Zahara NF, Mohamood T, Zainuddin N, Ayob MA, Tan SW (2018) Preparation, optimization and swelling study of carboxymethyl sago starch (CMSS)–acid hydrogel. *Chem Cent J* 12:133
31. Sabaa MW, Abdel Magid EH, Mohamed RR (2017) Maize starch-g-poly(n-vinylimidazole) synthesis and its application in sewage water treatment. *RRJCHEM* 6(2):55–67
32. Bauer AW et al (1966) Antibiotic susceptibility testing by a standardized single disc method. *Amer J Clin Pathol* 45:493–496
33. Dauletov Y et al. (2019) Copolymers of diallyldimethylammonium chloride and vinyl ether of monoethanolamine: synthesis, flocculating, and antimicrobial properties, 22nd international Symposium on Surfactants in Solution (SIS 2018), 22: 1129–1137
34. dos Santos RLO (2019) Antifungal efficiency of chemically and thermally-activated acrylic resins after surface treatment using poly (diallyldimethylammonium chloride). *Rev Soc Bras Med Trop.* <https://doi.org/10.1590/0037-8682-0033-2019>

**Publisher's Note** Springer Nature remains neutral with regard to jurisdictional claims in published maps and institutional affiliations.